JACS
JOURNAL OF THE AMERICAN CHEMICAL SOCIETY
Article
pubs.acs.org/JACS

Water Dynamics in Cytoplasm-Like Crowded Environment Correlates with the Conformational Transition of the Macromolecular Crowder

Pramod Kumar Verma,[†,‡] Achintya Kundu,[†,‡] Jeong-Hyon Ha,[§] and Minhaeng Cho*[,†,‡]

[†]Center for Molecular Spectroscopy and Dynamics, Institute for Basic Science (IBS), Seoul 02841, Republic of Korea
[‡]Department of Chemistry, Korea University, Seoul 02841, Republic of Korea
[§]Space-Time Resolved Molecular Imaging Research Team, Korea Basic Science Institute, Seoul 136-075, Republic of Korea

Supporting Information

ABSTRACT: Polyethylene glycol (PEG) is a unique polymer material with enormous applicability in many industrial and scientific fields. Here, its use as macromolecular crowder to mimic the cellular environment *in vitro* is the focus of the present study. We show that femtosecond mid-IR pump−probe spectroscopy using three different IR probes, HDO, HN_3, and azido-derivatized crowder, provides complete and stereoscopic information on water structure and dynamics in the cytoplasm-like macromolecular crowding environment. Our experimental results suggest two distinct subpopulations of water molecules: those that interact with other water molecules and those that are part of a hydration shell of crowder on its surface. Interestingly, water dynamics even in highly crowded environment remains bulk-like in spite of significant perturbation to the tetrahedral H-bonding network of water molecules. That is possible because of the formation of water aggregates (pools) even in water-deficient PEGDME-water solutions. In such a crowded environment, the conformationally accessible phase space of the macromolecular crowder is reduced, similar to biopolymers in highly crowded cytoplasm. Nonetheless, the hydration water on the surface of crowders slows down considerably with increased crowding. Most importantly, we do not observe any coalescing of surface hydration water (of the crowder) with bulk-like water to generate collective hydration dynamics at any crowder concentration, contrary to recent reports. We anticipate that the present triple-IR-probe approach is of exceptional use in studying how conformational states of crowders correlate with structural and dynamical changes of water, which is critical in understanding their key roles in biological and industrial applications.

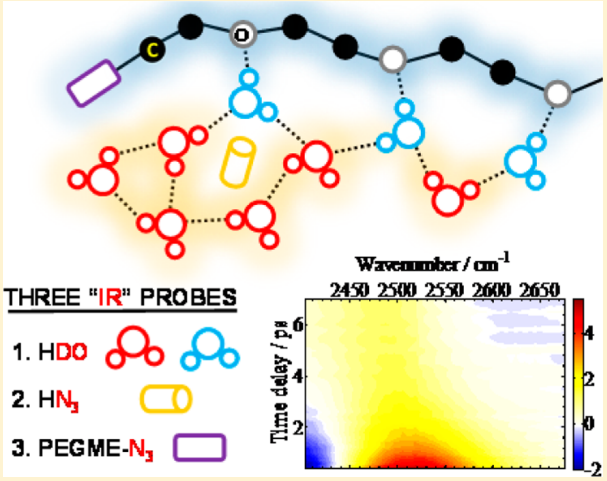

INTRODUCTION

Polyethylene glycol (PEG) is one of the most extensively studied synthetic polymers because of its various chemical, biological, medical, environmental, and industrial applications. Some of its important uses are as ion-conducting medium in polymer electrolyte batteries, for crystallizing proteins and nucleic acids, for purification of biological materials, as matrices for pharmaceutical drugs and devices, as edible films for food coating, and as lubricants in metal processing, among others.[1−4] All these uses are possible because of its flexible structure, very high water solubility, nonreactivity, low toxicity, and biodegradability.

Its very high water miscibility at moderate temperature has sparked numerous studies such as viscosity measurements,[5,6] conductometery,[7] NMR,[8−10] dielectric relaxation spectroscopy,[11] quasi-elastic neutron scattering,[12,13] Raman and infrared (IR) spectroscopies,[14−17] and molecular dynamics simulations[18−20] of PEG−water solutions. They suggest that PEG chain can adopt various conformations around C−C and C−O bonds of O−C−C−O unit segment. The trans−gauche−trans (*tgt*) conformation in the O−C−C−O segment adopted by solid PEG has been reported to be present even in PEG−water mixtures.[18,19,21−23] The *tgt* conformation is a basic unit of $^7/_2$ (seven chemical units and two turns) helical segment formed in PEG chains as confirmed by X-ray diffraction study.[24] For the helical conformation of PEG, the closest oxygen−oxygen distance is similar to that between neighboring water molecules in water.[25] The change of conformation, such as C−C bonds with a trans conformation and C−O bonds with a gauche confirmation, causes the helical structure to become random-coil so that both helical and random-coil-like conformers could coexist in solution.[18,19,21,22] PEG's ability to alter its local dipole moment by dihedral rotations along the C−C and C−O bonds modifies not only its conformations but also its interaction with surrounding molecules. This could be the reason why the number of water molecules hydrating a unit segment of PEG varies from 1 to 4.[7,10,14,16] The surface hydration water of PEG

Received: September 28, 2016
Published: November 18, 2016

ACS Publications © 2016 American Chemical Society

DOI: 10.1021/jacs.6b10164
J. Am. Chem. Soc. 2016, 138, 16081−16088

is known to form particular structured hydration shell because spacing of the ether oxygens of PEG, unlike those of polymethylene or polypropylene glycol, more or less matches with that of water−water H-bond geometry.[25] This PEG−water interaction is important because when contact occurs between PEG and a biological or chemical species they share common hydration layers and because those water molecules in the layers would play an important role in the function and stability of biological species or polymer.[26−28] Hence, studying water dynamics alone would not provide a complete picture of such biologically important systems in crowded environment.[17]

Being an artificial crowding agent, PEG when added to solution has been used to mimic the influence of crowders on water and biomolecules in cellular environment *in vitro*.[29,30] Crowding not only amplifies the complex interactions when hydration water layers overlap within several nanometer distances off the biomolecule surface but also modifies the protein intermolecular forces (when reducing the protein intermolecular distances) by way of entropic, excluded volume effects.[31,32] The perturbation to water by the crowders could have significant implications in cellular environments where the structural and dynamic correlation lengths may extend beyond the thickness of interstitial water layers. Thus, we have focused on both the water and the crowder itself, the subject of this study and a factor that has not been the subject of the focus to date. The queries that we seek to answer are what happens to water structure as the crowding is increased, whether water dynamics slow down, how does the crowder accommodate itself in such a crowded environment, and most importantly, is there any dynamical transition above a certain crowding threshold concentration as reported by King et al.[33] Note that they carried out 2D-IR experiments to study spectral diffusion dynamics of a covalently linked metal carbonyl IR probe to the surface of lysozyme in different concentrations of either PEG400 (average molecular weight of 400) or lysozyme and found that at around 60% PEG there appears a transition in the hydration dynamics as well as the protein dynamics. The question of whether this transition is a general phenomenon or a protein specific one was recently addressed by Hunag et al., and they did not find any protein hydration shell of γS-Crystallin that directly responds to crowding, using Overhauser dynamic nuclear polarization (ODNP).[34] Like other NMR techniques, ODNP is not highly sensitive to subpicosecond water dynamics. Hence, we here employ femtosecond (fs) mid-IR pump−probe (PP) technique to test whether a small solute (highly sensitive to water H-bonding) responds to the crowding or not. The model crowder that we chose to investigate is poly(ethylene glycol) dimethyl ether (PEGDME) shown in Scheme 1. PEGDME does not have terminal hydroxyl groups, so our model system is devoid of contribution from water−alcohol interactions.

To have a detailed microscopic picture of the crowded system, we employ three different vibrational (IR) probes (see Scheme 2). One probe is the well-known OD stretch mode of HDO that provides information on water structure from the water's point of view.[35−39] The other probes are azido (NNN) stretch modes of both hydrazoic acid (HN_3) and PEGME-N_3 (poly(ethylene glycol) methyl ether azide shown in Scheme 1). The former provides information from the dissolved solute's point of view and allows a direct assessment of how water's choice of H-bonding partner is altered upon crowding.[40] The latter furnishes how the crowder itself behaves with increased crowding. Our multiple-IR-probe approach thus enables us to have stereoscopic and complementary views on both structure and dynamics of water and crowder as well as correlation between them.

Scheme 1. Molecular Structures of Poly(ethylene glycol) Dimethyl Ether and Its Azido (NNN) Derivative[a]

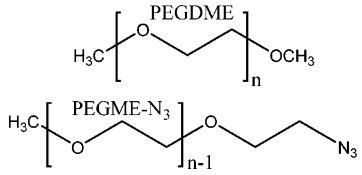

[a]A number-average molecular weight of 1000 corresponds to approximately 21 (n) ethylene oxide (labeled as "e") monomer units.

Scheme 2. Cartoon Representation of Water-Abundant and Highly Crowded PEG−Water Solutions with Three Independent Vibrational Probes

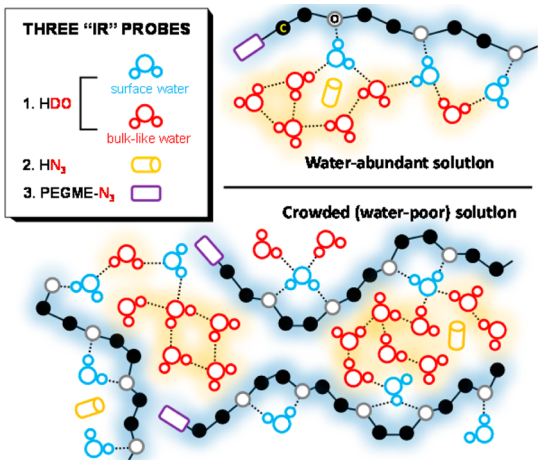

RESULTS AND DISCUSSION

Linear Spectra. Figure 1 shows the FTIR spectra of HDO, HN_3, and PEGME-N_3 in different wt % of crowder. Crowding causes a blue-shift (shifts to higher wavenumber) of OD band over a 76 cm^{-1} range with significant line-narrowing observed on the red side and relatively weaker broadening on the blue side of the spectrum (Figure 1A). Such asymmetric shifts in the low- and high-frequency sides of the spectra result not only from redistribution of equilibrium H-bond numbers and H-bonding strengths but also increased population of OD group H-bonded to ether oxygen of PEGDME, which will be denoted as OD-e.[17] The considerable narrowing on the red side indicates significant perturbation to the tetrahedral H-bonding network of water. However, the increased absorbance on the blue side of the spectrum is attributable to the increased OD-e population; note that the reduced electric field along the OD bond of HDO bound to ether oxygen atom increases the OD stretch frequency much like the cases of HDO molecules bound to anions in salt solutions.[41]

Unlike the OD band, the azido stretch mode of both solute (HN_3) and crowder (PEGME-N_3) undergo substantial red-shifts (shifts to lower wavenumber) with increased crowding (Figures 1D,G). This can be explained by noting that at high crowder concentration water prefers to make H-bonds with PEGDME ether oxygen (e) instead of HN_3 (solute); furthermore, the solute can only make H-bonding interaction with those water molecules that are part of partially broken H-

DOI: 10.1021/jacs.6b10164
J. Am. Chem. Soc. 2016, 138, 16081−16088

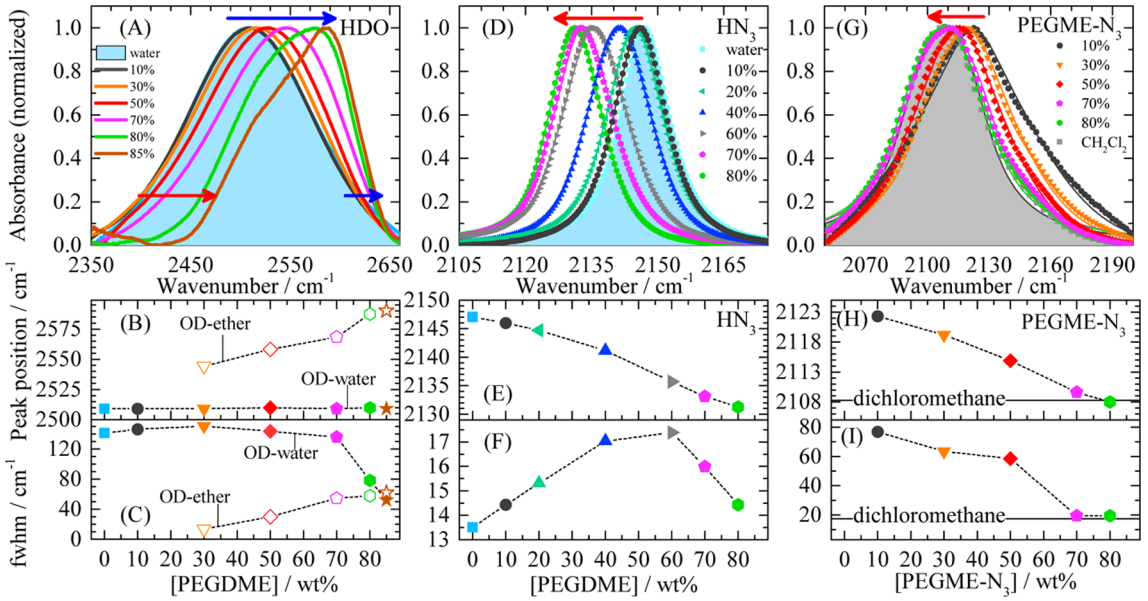

Figure 1. FTIR absorption spectra of the OD stretch of HDO (A) along with their peak positions (B) and fwhm (full-width at half-maximum) (C) in different wt % of crowder. FTIR (HDO) spectrum at each crowder concentration (except 10 wt %) was fitted with a Gaussian function with two different peaks, corresponding to OD-water (OD-w, fixed at ~2509 cm^{-1}) and OD-ether (OD-e), respectively (Figure S1). Azido stretch IR spectra (D and G); symbols are raw data and lines are fit, obtained by fitting raw data with pseudo-Voigt function) of HN_3 and PEGME-N_3 along with their peak positions (E and H) and fwhm values (F and I) with respect to crowder wt %. Blue shaded area is for neat water, while gray one is for dichloromethane. The dashed lines are guides to the eye.

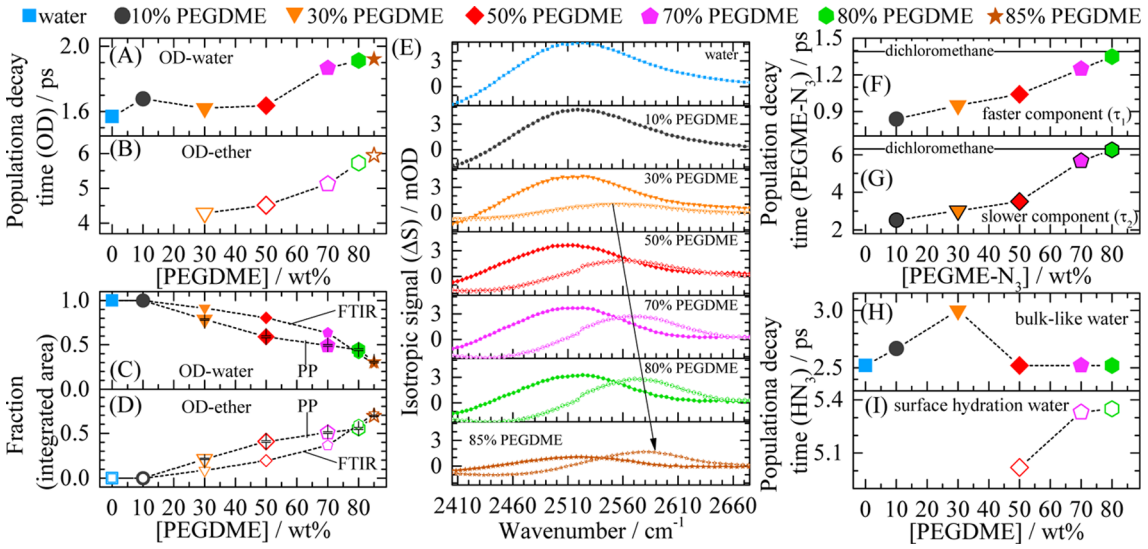

Figure 2. Vibrational lifetime of the OD stretch mode of HDO (A and B) and its amplitude (C and D) as a function of crowder wt %. The population relaxation is single exponential below 30 wt %, above which it is biexponential (OD-w and OD-e). Crowding does not slow down the vibrational relaxation of OD stretch mode of HDO interacting with water, though its fraction (obtained from the integrated area of decomposed PP signal (E)) decreases. Population relaxation of azido stretch mode of PEGME-N_3 (F and G) decays biexponentially (τ_1 and τ_2) in dichloromethane and at all crowder concentrations. With decrease in water amount, both lifetimes approach a value close to that in dichloromethane with sudden increase above 60 wt % of crowder. Population relaxation of azido stretch mode of HN_3 (H and I) decays in a single exponential manner until 30 wt %, above which appears a slow component similar to what has been observed inside small reverse micelle with nanometer-sized water pool. Details of the heating correction procedure (if required) are presented in Supporting Information. The dashed lines are guides to the eye.

bonding network.[42] What is more interesting is the increase in the line width (fwhm) of the azido band of HN_3 up to 60 wt % PEGDME, which is then followed by a sudden decrease (Figure 1F) upon further increase in PEGDME concentration. The increase in width in the concentration range from 0 to 60 wt % PEGDME means that the solutes' solvation shell becomes increasingly heterogeneous due to different types of H-bonded subpopulations at molecular level. However, as the PEGDME concentration further increases beyond 60 wt %, the solute HN_3 experiences relatively homogeneous environment, suggesting a conformational change of PEGDME at around 60 wt % PEGDME (Figure 1F).[10,15,21] This is further confirmed by the observation that the width of the azido stretch band of PEGME-N_3 at higher concentration (>60 wt %) reaches an asymptotic value that is close to the bandwidth of PEGME-N_3 in dichloromethane (water less environment) (Figure 1I). The

DOI: 10.1021/jacs.6b10164
J. Am. Chem. Soc. 2016, 138, 16081−16088

decrease in bandwidth of the azido stretch band of PEGME-N_3 with increased crowding indicates that the conformationally accessible states of the macromolecular crowder are being restricted, which is similar to what they do to biomolecules in crowded environments.[30]

Vibrational Population Relaxation. Vibrational lifetime is highly sensitive to local environment because vibrational energy relaxation (VER) depends on the coupling of the excited vibrational mode to intra- and intermolecular accepting modes and their densities of states.[43] Vibrational probe in different local environments will have different coupled intramolecular modes and will experience different bath density of states. The isotropic PP spectra (Figures S2−S4) of either HDO (water) or HN_3 (water) or PEGME-N_3 (dichloromethane) consist of a positive (0−1 transition) ground-state bleach (GSB) and stimulated emission (SE) peaks near 2520, 2147, and 2105 cm^{-1} and a negative (1−2 transition) excited-state absorption (ESA) peaks at wavenumbers below 2430, 2116, and 2072 cm^{-1}, respectively.

Water's Point of View. In femtosecond mid-IR pump−probe experiment, we excite the 0−1 vibration of an IR-active probe, e.g., OD stretch of HDO. Subsequently, the initially excited mode (OD stretch) deposits its energy through different paths into a combination of other modes so that the energy is conserved. These energy relaxation pathways involve high-frequency modes of water and other interacting molecules (PEGDME) such as HDO bends and low-frequency bath modes, such as intermolecular hindered transitional and librational modes. In aqueous solutions of PEGDME, HDO can interact with other water hydroxyl groups (OD-w) and also with ether oxygen of PEGDMEs (OD-e). In the case where the OD group is H-bonded to water, it will be coupled differently to a distinct set of intramolecular modes and a different density of states than that H-bonded to ether oxygen of PEGDME. In essence, the vibrational relaxation of the OD stretch will therefore be very sensitive to the local (H-bonding) environment. In neat water (Figure 2A), we obtain a time constant of 1.6 ps for the vibrational lifetime of OD stretch on fitting the PP data (see Supporting Information for details).[41] In dilute (water-abundant) solutions (<30 wt % PEGDME), the population decay is still monoexponential with time constant similar to that of HDO in neat water despite the fact that there are two subpopulations of HDO, i.e., OD-w and OD-e. The apparent monoexponential decay suggests not only that the OD-e subpopulation is relatively small but also that OD-e regions are still water-rich (water molecules hydrating ether oxygen atoms are connected to other water molecules), e.g., at 10 wt % PEGDME, 349 water molecules are available per PEGDME (16 water per ether) (see the upper panel of Scheme 2). For PEGDME concentration ≥30 wt %, the population decay of OD stretch mode can only be fit with a biexponential function. The fast component (<2 ps) corresponds to the bulk-like water (OD-w), while the slow (>4 ps) relates to the OD-e. At 30 wt % PEGDME, there are 90 water molecules per PEGDME (4 water molecules per ether), which decreases to 10 (less than 1 water per ether) at 80 wt % PEGDME. The decomposed isotropic PP spectra of the bulk-like water component (OD-w) and the OD-e are shown in Figure 2E from 30 wt % PEGDME onward (vide infra).

One of the most important observations is that the decay time of the fast component (OD-w) is negligibly dependent on crowder concentration (Figure 2A). Even in 85 wt % PEGDME−water solution, 34% component of the relaxation occurs on a time scale similar to that in neat water. This bulk-like water at all crowder concentrations in part confirms the finding of King et al., where they did not find any PEG400 dependence of vibrational relaxation of metal carbonyl IR probe that is covalently attached to the surface of lysozyme.[33] Although in our findings the water−water network (through H-bonding) is strongly perturbed by PEGDME (FTIR), there exist large-size water aggregates (pools), and VER of HDO in such water aggreates remains unaffected by PEGDME. This is in stark contrast to an NMR (spin−lattice relaxation times of proton) study where the authors suggested that water dynamics is always affected by PEG at any PEG concentration.[44] Note that NMR is not very sensitive to subpicosecond water dynamics. Our results provide direct evidence of water aggregates (pool) formation even in highly crowded environment. This is extremely crucial for maintaining function and solubility of biomolecules in cytoplasm-like crowded environments.

Unlike the fast component (OD-w), the decay time of the slow component (OD-e) becomes increasingly slower with increased crowding (Figure 2B). This implies that the local contact (H-bonding) interaction and structure of the OD-e change upon decreasing the number of available water molecules. As mentioned earlier, less than one water per ether is present in highly crowded solutions (70−85 wt % PEGDME). If all the water molecules interact with ether oxygen atoms, then there would only be OD-e species resulting in a monoexponential decay of isotropic PP data. However, that is not the case observed here, as there remain water aggregates (pools) in highly crowded solutions. Hence, there must occur conformational change in PEGDME because of its ability to adopt different conformers as solvating water concentration is lowered.[21,22] The structural change could be related to an increasing heterogeneity in the conformations of the O−C−C−O segments such as a greater mixture of *tgt*, *ttg*, or *ttt* backbone conformations. Direct evidence of considerable structural change in PEGDME at around 60 wt % of crowder can be seen in a sudden change (decrease) of the fwhm in FTIR spectra of PEGME-N_3 (Figure 1I). It is believed that above that concentration the PEG has restricted conformational freedoms or phase space.

Analysis of the FTIR Spectra with Two-Component Model. The analysis of the isotropic PP spectra reveals two subpopulations with distinctively different vibrational lifetimes (OD-w and OD-e). The peak position of the OD-w isotropic PP spectrum does not change much, but that of the OD-e shifts to higher wavenumber with increased crowding (Figure 2E). Hence, we fitted the FTIR spectra of the OD stretch band with a Gaussian function with two different peaks, one fixed at ∼2509 cm^{-1} corresponding to OD-w subpopulation. The population of both the OD-w and OD-e obtained from the integrated areas of the corresponding PP eigen-spectra as well as FTIR spectra are plotted together in Figure 2C,2D. There are some deviations in the population fractions estimated from FTIR and PP data especially at intermediate concentrations where the structural heterogeneity is maximum as discussed earlier. Nonetheless, the overall agreements are quantitative.

Crowder's Point of View. Next, we examine the information content extracted from azido probe covalently attached to the crowder, PEG itself (Scheme 1). In dichloromethane (water absent), there are two decay components of the azido stretch mode in PEGME-N_3, which are 1.4 and 6.3 ps (Figure 2F,G).[45] In water-abundant solutions, both the fast and

DOI: 10.1021/jacs.6b10164
J. Am. Chem. Soc. 2016, 138, 16081−16088

slow time components become much faster, reflecting the unique sensitivity of the azido stretch mode to local H-bonding interaction.[45,46] There is marginal but noticeable increase in both the lifetimes until 50 wt % crowder; however, above this they both reach values that are close to those of PEGME-N_3 in dichloromethane. This provides an important clue about conformational transition of PEGDME upon decreasing water concentration. In water-abundant PEGDME-water solutions, excluded volume effects are predominantly intramolecular so that crowders and water cooperate to form a highly linked network that allows the hydrocarbon groups to be reasonably encaged in the interstitial space and the PEG chain remains extended and hydrated (Scheme 2). As water content decreases, intermolecular excluded volume interactions cause crowders to share their hydration shells with others and adopt crystalline structure similar to solid PEG where its contacts with water are minimized but optimized. This enhanced intermolecular interaction favors helical conformation of PEGDME and water pooling (Scheme 2).

Solute's Point of View. To investigate crowding effect on water-sensitive solute molecules, we used the azido stretch mode of HN_3, which is an excellent vibrational probe reporting the amount of water available to chemical groups, e.g., peptides and amino acids, of biomolecules.[46−49] The vibrational lifetime of HN_3 is plotted in Figure 2H as a function of crowder wt %. In water-rich solutions (10−30 wt % PEGDME), water−water or water−ether contacts are most likely interacting with another water molecule through extended H-bonding, a feature unique to water (see the upper panel in Scheme 2). In these dilute (less crowded) solutions, though the local heterogeneity is high; the diversity in the H-bonding capability seems to increase the vibrational lifetime of HN_3 marginally. However, from 50 wt % onward, the VER process of HN_3 is no longer describable with a single exponentially decaying function, and there newly appears a slow component (>5 ps) along with the faster one (<3 ps). The fast relaxation time corresponds to HN_3 molecules in bulk-like water environment because the vibrational lifetime of HN_3 in pure water is known to be 2.5 ps.[50] The slow relaxation time in highly crowded solutions arises from the solute's contact with the hydration water on the crowder surfaces. Our earlier studies have shown that VER of HN_3 in reverse micelles with nanometer water pool is very slow (>6 ps) because HN_3 is mostly surrounded by interfacial water.[50] The other possibility is that HN_3 has no water contact within the hydration shell or in PEGDME segment, but in that case the lifetime would be 8 ps and higher (vibrational lifetime of HN_3 in toluene and dichloromethane are 8.1 and 20.5 ps, respectively; unpublished work). Clear separation of water aggregates (pools) and PEGDME-surface water in 50 wt % (PEGDME) and above is a very important observation that the coalescing of bulk-like and surface hydration water does not occur with macromolecular crowding (PEGDME). This is in stark contrast to a recent 2D-IR study where sharp convergence of hydration and bulk water above a certain crowding (PEG400) threshold concentration was observed with covalently attached metal carbonyl IR probe to the surface of lysozyme.[33] These seemingly contrary observations can be understood by considering that macromolecular crowding is not a general phenomenon but rather a specific one depending on solute (or protein) size and type.[34] The Kubarych group also reported that the vibrational lifetime of metal carbonyl attached to the surface of lysozyme is insensitive to PEG400 concentration. One possible reason for such insensitivity of vibrational lifetime of metal carbonyl could be the large size of IR probe molecule, which mostly facilitates the coupling of the excited vibrational mode to intra- rather than intermolecular accepting modes. Small vibrational probes such as HN_3 and cyano-phenylalanine molecular probes exhibit pronounced change in lifetime just upon isotope substitution.[51,52]

Orientational Relaxation. Polarization-selective femtosecond mid-IR pump−probe measurement allows us to extract not only the population releaxation but also the orientational relaxation parameters (see Experimental Section). Orientational relaxation of water involves concerted breaking and reforming of H-bonds of the water molecule in bifurcated H-bond configuration with two other water molecules (incoming and outgoing). Any hindrance to such processes either by reduced number of H-bond partners or excluded volume effect by any neighboring molecule to the incoming water partner will slow down the relaxation.[53] For HDO in neat water, the anisotropy $r(t)$ decays exponentially with a time constant of 2.3 ± 0.2 ps (Figure 3A).[41] In neat water, complete orientational relaxation

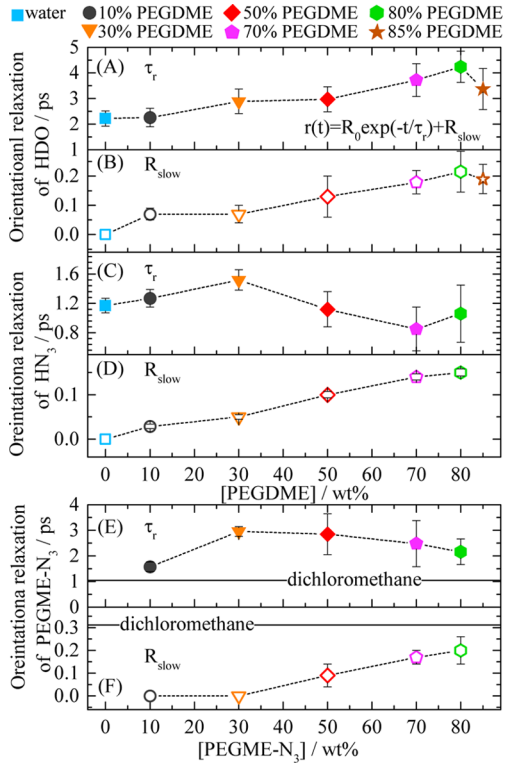

Figure 3. Concentration dependence of rotational relaxation times of HDO (A), HN_3 (C), and PEGME-N_3 (E). The anisotropy decays were fitted to a single exponential function (with time constant of τ_r) with an offset (R_{slow}), and the fits were carried out at the center of either the OD band or azido bands of HN_3 and PEGME-N_3. Individual fitting results of the anisotropy data of HDO, HN_3, and PEGME-N_3 are shown in Figures S5−S7. The dashed lines are guides to the eye.

involves a concerted dynamics of many molecules because any water molecule is connected to multiple water molecules through H-bonds. Addition of PEGDME produces a very slow reorientation component whose amplitude increases with crowder concentration. The slow component (>10 ps) is modeled as an offset in the anisotropy decay ($r(t) = R_0 \exp(-t/\tau_r) + R_{slow}$). The increase in τ_r (OD-w) with crowder concentration is due to the reduction in average H-bond number of water molecules. The slower component (R_{slow})

DOI: 10.1021/jacs.6b10164
J. Am. Chem. Soc. 2016, 138, 16081−16088

corresponds to ether oxygen-bound water subpopulation (OD-e) where the excluded volume effect by PEG, rather than the average number of H-bond, plays a major role in slowing down the relaxation in this case.

A similar conclusion can also be drawn from fitting the anisotropy decay of HN_3. The amplitude of R_{slow} progressively increases with the crowder concentration (Figure 3D). R_{slow} represents the relative fraction of HN_3 molecules interacting mostly with surface hydration water of the crowder. However, τ_r of HN_3 does not change much with crowding (Figure 3C) unlike τ_r of HDO. Note that HDO can make multiple H-bonds to other water molecules, but HN_3 preferentially makes a single H-bond with a water molecule. Therefore, any reduction in average H-bond number of HDO would affect the OD rotational dynamics significantly more than that of HN_3 to its rotational dynamics.[40]

We also measured anisotropy of PEGME-N_3 in dichloromethane and found that the decay has a fast component (of approximately 1 ps) and a huge offset (R_{slow}). This clearly suggests a wobbling-in-a-cone mechanism, where the fast component arises from the azido group (covalently attached to the tail segment of the crowder) wobbling around within a limited cone of angles.[54] The restricted wobbling of the azido transition dipole contributes to the anisotropy decay but does not result in its complete decay. The huge offset in the anistropy decay (Figure S7, topmost) suggests that the PEGME-N_3 in water-lacking environment has restricted conformational flexibility with fairly compact structures. Interestingly, the anisotropy of PEGME-N_3 decays almost completely in 10 wt % of crowder, which manifests that the crowder in extended and fully hydrated state (especially with flexible tail segment) undergoes fast and large structural fluctuations in relatively less crowded solutions. With decreasing water content, the τ_r increases followed by marginal decrease. In addition, the R_{slow} component appears at 50 wt % and onward, and its amplitude rises until 80 wt % of crowder. However, even at this lowest water concentration, the amplitude of R_{slow} is less than that in dichloromethane solution. As suggested by other works, the PEGDME adopts conformationally mixed segments at dilute and intermediate concentrations with extended and sufficiently hydrated (ether oxygen) chains as they actively participate in extensive H-bonding network of water (Scheme 2) because the spacing of the ether oxygens of PEG matches with the water−water H-bond geometry.[10] In water-poor solutions (70−80 wt %) however, PEG favors a compact helical structure, which is similar to that of crystalline PEG, with some random-coil segments.[21,22]

Conformational Transition of PEG. To support these findings on the interplay of PEGDME conformational transition with water structure and dynamics upon increasing crowder concentration, we further compared the C−H stretching vibrations of PEGDME at ∼2919 cm^{-1} (associated with random-coil configuration of PEGDME) and ∼2883 cm^{-1} (both random-coil and *tgt* conformations of PEGDME) (Figure 4).[21−23] The recorded FTIR spectra at 85 wt % has the highest intensity at ∼2885 cm^{-1} similar to what is observed in solid PEG.[21] In addition, the peak around 2918 cm^{-1} is also present, representing some random-coil segments. As the water concentration increases, the ratio of absorbance at 2883 cm^{-1} to that at 2919 cm^{-1} decreases, indicating a decrease of the population of helical segments. Interestingly, a significant structural change seems to occur close to 60 wt % (Figure 4), which in turn modifies the interaction between the water and ether oxygen corroborating with our fs mid-IR PP measurements.

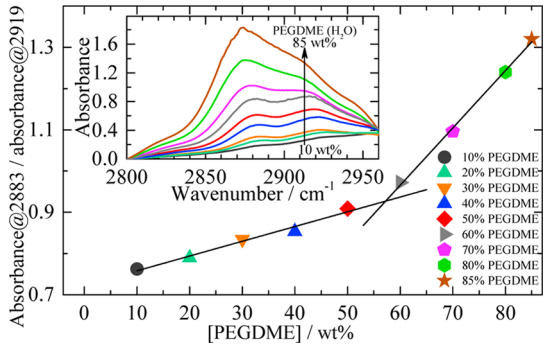

Figure 4. Crowder wt % dependence of the ratio of absorbance of C−H stretch mode at 2883 cm^{-1} to that at 2919 cm^{-1} from the FTIR spectra (inset). The peak at ∼2919 cm^{-1} corresponds to the C−H stretching vibrations of PEG with a random-coil component, and the component at ∼2883 results from the C−H stretching vibrations of PEG with both random-coil and *tgt* (trans−gauche−trans) conformations. The solid lines are fitted to a straight line in water-rich solutions (10−50 wt %) and water-poor solutions (70−85 wt %) revealing a probable preference to helical (*tgt*) conformation at PEGDME concentrations higher than 60 wt %.

CONCLUSIONS

Here, our triple-IR-probe approach with fs mid-IR polarization selective PP measurements has been shown to be exceptionally useful to elucidate the underlying crowding effects not only on water structure and dynamics but also on crowder itself. Crowding is a crucial phenomenon found in a variety of cellular environments. The crowder itself feels the excluded volume effect that it also imposes on protein. This happens because PEG can modify the nature of interaction between its ether oxygen and water. In dilute (water-rich) solutions, the PEG adopts a relaxed conformation with mixed random-coil and helical structures, but the local heterogeneity increases as water content decreases in a macromolecular-crowding environment. As PEG concentration further increases beyond a certain threshold (∼60 wt %), conformational distribution of PEG changes considerably by adopting compact and presumably helical structure, much like that in crystalline solid PEG. Our results show that the crowding does perturb the (H-bond) networking feature of water molecules with at least two subpopulations of water: bulk-like (OD-w) and surface hydration water (OD-e). The interstitial water dynamics remain bulk-like, even in a highly crowded environment. It is only the surface hydration water dynamics that slow down upon increased crowding especially in water-deficient solutions. Therefore, our experimental data does not support the assertion that water in highly crowed solutions like cytoplasm behaves completely differently from bulk water.[55] Furthermore, we do not observe any coalescing of bulk-like and surface hydration water with PEGDME as crowder, i.e., there is no abrupt change in water dynamics associated with collective hydration. A far-reaching impact of this study is that the macromolecular crowding has just a marginal influence on water dynamics, and water-sensitive solutes remain hydrated mostly by bulk-like water. This supports the notion that the effect of macromolecular crowding depends on the stability of the protein-specific and−intrinsic hydration shell. We further anticipate that studying the properties of such highly crowded

DOI: 10.1021/jacs.6b10164
J. Am. Chem. Soc. 2016, 138, 16081−16088

solutions can shed light on properties of water inside living organisms.

EXPERIMENTAL SECTION

Sample Preparation and FTIR Measurement. Poly(ethylene glycol) dimethyl ether (CAS No. 24991−55−7), poly(ethylene glycol) methyl ether azide (CAS No. 89485−61−0), sodium azide (CAS No. 26628−22−8), deuterium oxide (CAS No. 7789−20−0), and Amberlyst 15 (hydrogen form; CAS No. 39389−20−3) were purchased from Sigma-Aldrich and used as received. Double-distilled water was used in preparation of isotopically diluted water (5% v/v HDO in H_2O) and other aqueous solutions. HN_3 was prepared by using ion-exchange method. A 1.5 M aqueous solution of sodium azide was passed through a column of Amberlyst 15 resin to obtain HN_3 (identified by its absorption peak near 2147 cm^{-1}). Different wt % of crowder solutions were prepared by mixing the appropriate weight of crowder either with isotopically diluted water or aqueous solution of hydrazoic acid. The resulting solutions were vortexed and sonicated to obtain a clear solution. Throughout this paper, we use the wt % (w/w) concentration of crowder.

FTIR absorption spectra were collected by using the VERTEX70 FTIR spectrometer (Bruker Optics) with 1 cm^{-1} resolution. Separate spectra were collected for all wt % of crowder solutions for background-correction purposes. The measurements were performed at room temperature. The sample solutions were housed in a homemade cell with two CaF_2 windows. The thickness of CaF_2 windows were 2 and 3 mm for FTIR and PP measurements, respectively. The cell path length was varied by using a Teflon spacer (Harrick Scientific Products Inc.) of different thickness (12, 25, and 56 μm). The absorbances of OD and NNN vibration bands were kept in the range of 0.3 to 0.5 for subsequent femtosecond mid-IR PP measurements by using the Teflon spacer of appropriate thickness.

Polarization-Controlled Femtosecond Mid-IR Pump−Probe Spectroscopy. An optical parametric amplifier converts the output beam of a Ti:sapphire oscillator/regenerative amplifier (Tsunami, Spitfire; Spectra Physics) into two near-IR pulses centered at ∼1.4 and ∼1.9 μm. The resulting signal and idler pulses were difference-frequency-mixed in $AgGaS_2$ so that mid-IR pulses with center frequency of either 2530 or 2130 cm^{-1} were produced, depending on the crystal position. A pair of CaF_2 plates of different thickness were used to compensate for the linear dispersion introduced by other dielectric materials in the setup. The nearly transform limited mid-IR pulses were split into pump and probe by a ZnSe beam splitter. The pump beam was chopped (500 Hz) by an optical chopper electronically synchronized with the laser system. The delay between pump and probe pulses was controlled by changing beam path length of the probe beam through a delay stage. Both pump and probe were linearly polarized and the polarization of the probe beam was adjusted by a polarizer to have its polarization to be 45° with respect to the pump polarization. After the sample, the parallel and perpendicular component of the probe were alternatively selected by an additional motorized polarizer, and the selected probe beam was directed to another polarizer placed before the monochromator to match the intensity of parallel or perpendicular probe beam onto the 64-element MCT (Mercury Cadmium Telluride) array detector. Every two pulses (with and without pump) were collected for each probe polarization. After subtracting the unpumped signal from the pumped at each delay time t, we obtain the parallel ($\Delta S_{\parallel}(t)$) and perpendicular ($\Delta S_{\perp}(t)$) signals. The isotropic signals are constructed from the parallel ($\Delta S_{\parallel}(t)$) and perpendicular ($\Delta S_{\perp}(t)$) signals using the equation $\Delta S_{iso}(t) = (\Delta S_{\parallel}(t) + 2\Delta S_{\perp}(t))/3 \cdot \Delta S_{iso}$ provides information on the vibrational population relaxation of the vibrationally excited state and is independent of molecular reorientation. The anisotropic signal is calculated from the normalized difference signals between $\Delta S_{\parallel}(t)$ and $\Delta S_{\perp}(t)$, i.e., $r(t) = (\Delta S_{\parallel}(t) - \Delta S_{\perp}(t))/(\Delta S_{\parallel}(t) + 2\Delta S_{\perp}(t))$, and decays with molecular reorientation rate that is directly proportional to the second Legendre orientational correlation function.

ASSOCIATED CONTENT

Supporting Information

The Supporting Information is available free of charge on the ACS Publications website at DOI: 10.1021/jacs.6b10164.

Experimental methods (fitting details and heat correction procedure, fitting quality of the FTIR data, representative isotropic PP data, and individual fitting of all the anisotropy decays for all the wt % of crowder) (PDF)

AUTHOR INFORMATION

Corresponding Author

*E-mail: mcho@korea.ac.kr.

ORCID

Pramod Kumar Verma: 0000-0001-8837-3167

Minhaeng Cho: 0000-0003-1618-1056

Notes

The authors declare no competing financial interest.

ACKNOWLEDGMENTS

This work was supported by IBS-R023-D1. All mid-IR PP measurements were performed in the Seoul center of Korea Basic Science Institute (KBSI).

REFERENCES

(1) Elia, G. A.; Hassoun, J. *Sci. Rep.* **2015**, *5*, 12307.
(2) McPherson, A. *Methods Enzymol.* **1985**, *114*, 120.
(3) Al-Hamarneh, I. F.; Pedrow, P. D.; Goheen, S. C.; Hartenstine, M. J. *IEEE Trans. Plasma Sci.* **2007**, *35*, 1518.
(4) The, D. P.; Debeaufort, F.; Luu, D.; Voilley, A. *J. Membr. Sci.* **2008**, *325*, 277.
(5) Devanand, K.; Selser, J. C. *Nature* **1990**, *343*, 739.
(6) Bailey, F. E.; Callard, R. W. *J. Appl. Polym. Sci.* **1959**, *1*, 56.
(7) Bordi, F.; Cametti, C.; Di Biasio, A. *J. Phys. Chem.* **1988**, *92*, 4772.
(8) Breen, J.; Huis, D.; de Bleijser, J.; Leyte, J. C. *J. Chem. Soc., Faraday Trans. 1* **1988**, *84*, 293.
(9) Connor, T. M.; McLauchlan, K. A. *J. Phys. Chem.* **1965**, *69*, 1888.
(10) Lüsse, S.; Arnold, K. *Macromolecules* **1996**, *29*, 4251.
(11) Huang, L.; Nishinari, K. *J. Polym. Sci., Part B: Polym. Phys.* **2001**, *39*, 496.
(12) Trouw, F. R.; Borodin, O.; Cook, J. C.; Copley, J. R. D.; Smith, G. D. *J. Phys. Chem. B* **2003**, *107*, 10446.
(13) Borodin, O.; Trouw, F.; Bedrov, D.; Smith, G. D. *J. Phys. Chem. B* **2002**, *106*, 5184.
(14) Koenig, J. L.; Angood, A. C. *J. Polym. Sci. A-2 Polym. Phys.* **1970**, *8*, 1787.
(15) Wahab, S. A.; Matsuura, H. *Phys. Chem. Chem. Phys.* **2001**, *3*, 4689.
(16) Liu, K.-J.; Parsons, J. L. *Macromolecules* **1969**, *2*, 529.
(17) Fenn, E. E.; Moilanen, D. E.; Levinger, N. E.; Fayer, M. D. *J. Am. Chem. Soc.* **2009**, *131*, 5530.
(18) Smith, G. D.; Bedrov, D.; Borodin, O. *J. Am. Chem. Soc.* **2000**, *122*, 9548.
(19) Lee, H.; Venable, R. M.; MacKerell, A. D., Jr; Pastor, R. W. *Biophys. J.* **2008**, *95*, 1590.
(20) Tasaki, K. *J. Am. Chem. Soc.* **1996**, *118*, 8459.
(21) Gemmei-Ide, M.; Miyashita, T.; Kagaya, S.; Kitano, H. *Langmuir* **2015**, *31*, 10881.
(22) Gemmei-Ide, M.; Motonaga, T.; Kasai, R.; Kitano, H. *J. Phys. Chem. B* **2013**, *117*, 2188.
(23) Shephard, J. J.; Bremer, P. J.; McQuillan, A. J. *J. Phys. Chem. B* **2009**, *113*, 14229.
(24) Tadokoro, H.; Chatani, Y.; Yoshihara, T.; Tahara, S.; Murahashi, S. *Makromol. Chem.* **1964**, *73*, 109.
(25) Kjellander, R.; Florin, E. *J. Chem. Soc., Faraday Trans. 1* **1981**, *77*, 2053.

DOI: 10.1021/jacs.6b10164
J. Am. Chem. Soc. 2016, 138, 16081−16088

(26) Zhang, Y.; Furyk, S.; Bergbreiter, D. E.; Cremer, P. S. *J. Am. Chem. Soc.* **2005**, *127*, 14505.
(27) Zhang, Y.; Cremer, P. S. *Curr. Opin. Chem. Biol.* **2006**, *10*, 658.
(28) Correa, N. M.; Silber, J. J.; Riter, R. E.; Levinger, N. E. *Chem. Rev.* **2012**, *112*, 4569.
(29) Verma, P. K.; Rakshit, S.; Mitra, R. K.; Pal, S. K. *Biochimie* **2011**, *93*, 1424.
(30) Reid, C.; Rand, R. P. *Biophys. J.* **1997**, *72*, 1022.
(31) Zhou, H.-X.; Rivas, G.; Minton, A. P. *Annu. Rev. Biophys.* **2008**, *37*, 375.
(32) Miklos, A. C.; Sarkar, M.; Wang, Y.; Pielak, G. J. *J. Am. Chem. Soc.* **2011**, *133*, 7116.
(33) King, J. T.; Arthur, E. J.; Brooks, C. L.; Kubarych, K. J. *J. Am. Chem. Soc.* **2014**, *136*, 188.
(34) Huang, K.-Y.; Kingsley, C. N.; Sheil, R.; Cheng, C.-Y.; Bierma, J. C.; Roskamp, K. W.; Khago, D.; Martin, R. W.; Han, S. *J. Am. Chem. Soc.* **2016**, *138*, 5392.
(35) Lawrence, C. P.; Skinner, J. L. *J. Chem. Phys.* **2002**, *117*, 8847.
(36) Kundu, A.; Błasiak, B.; Lim, J.-H.; Kwak, K.; Cho, M. *J. Phys. Chem. Lett.* **2016**, *7*, 741.
(37) Lee, H.; Choi, J.-H.; Verma, P. K.; Cho, M. *J. Phys. Chem. A* **2016**, *120*, 5874.
(38) Asbury, J. B.; Steinel, T.; Kwak, K.; Corcelli, S. A.; Lawrence, C. P.; Skinner, J. L.; Fayer, M. D. *J. Chem. Phys.* **2004**, *121*, 12431.
(39) Asbury, J. B.; Steinel, T.; Stromberg, C.; Corcelli, S. A.; Lawrence, C. P.; Skinner, J. L.; Fayer, M. D. *J. Phys. Chem. A* **2004**, *108*, 1107.
(40) Verma, P. K.; Lee, H.; Park, J. Y.; Lim, J. H.; Maj, M.; Choi, J. H.; Kwak, K. W.; Cho, M. *J. Phys. Chem. Lett.* **2015**, *6*, 2773.
(41) Omta, A. W.; Kropman, M. F.; Woutersen, S.; Bakker, H. J. *Science* **2003**, *301*, 347.
(42) Wolfshorndl, M. P.; Baskin, R.; Dhawan, I.; Londergan, C. H. *J. Phys. Chem. B* **2012**, *116*, 1172.
(43) Oxtoby, D. W. *Annu. Rev. Phys. Chem.* **1981**, *32*, 77.
(44) Clop, E. M.; Perillo, M. A.; Chattah, A. K. *J. Phys. Chem. B* **2012**, *116*, 11953.
(45) Lee, K.-K.; Park, K.-H.; Joo, C.; Kwon, H.-J.; Jeon, J.; Jung, H.-I.; Park, S.; Han, H.; Cho, M. *J. Phys. Chem. B* **2012**, *116*, 5097.
(46) Tucker, M. J.; Gai, X. S.; Fenlon, E. E.; Brewer, S. H.; Hochstrasser, R. M. *Phys. Chem. Chem. Phys.* **2011**, *13*, 2237.
(47) Kim, H.; Cho, M. *Chem. Rev.* **2013**, *113*, 5817.
(48) Taskent-Sezgin, H.; Chung, J.; Banerjee, P. S.; Nagarajan, S.; Dyer, R. B.; Carrico, I.; Raleigh, D. P. *Angew. Chem., Int. Ed.* **2010**, *49*, 7473.
(49) Choi, J.-H.; Raleigh, D.; Cho, M. *J. Phys. Chem. Lett.* **2011**, *2*, 2158.
(50) Lee, J.; Maj, M.; Kwak, K.; Cho, M. *J. Phys. Chem. Lett.* **2014**, *5*, 3404.
(51) Rodgers, J. M.; Zhang, W.; Bazewicz, C. G.; Chen, J.; Brewer, S. H.; Gai, F. *J. Phys. Chem. Lett.* **2016**, *7*, 1281.
(52) Houchins, C.; Weidinger, D.; Owrutsky, J. C. *J. Phys. Chem. A* **2010**, *114*, 6569.
(53) Laage, D.; Hynes, J. T. *Science* **2006**, *311*, 832.
(54) Fujiwara, T.; Nagayama, K. *J. Chem. Phys.* **1985**, *83*, 3110.
(55) Pollack, G. H.; Cameron, I. L.; Wheatley, D. N. *Water and the Cell*; Springer: Dordrecht, 2007.

DOI: 10.1021/jacs.6b10164
J. Am. Chem. Soc. 2016, 138, 16081−16088